Infrared Multiphoton Dissociation Spectroscopy of Gas-Phase Mass-Selected Hydrocarbon–Fe + Complexes

ARTICLE *in* JOURNAL OF THE AMERICAN CHEMICAL SOCIETY · OCTOBER 2004

Impact Factor: 12.11 · DOI: 10.1021/ja0488176 · Source: PubMed

6 AUTHORS, INCLUDING:

Aude Simon
Paul Sabatier University - Toulouse III
21 PUBLICATIONS **425** CITATIONS
SEE PROFILE

Joel Lemaire
Université Paris-Sud 11
109 PUBLICATIONS **2,630** CITATIONS
SEE PROFILE

Philippe Maître
Université Paris-Sud 11
141 PUBLICATIONS **3,566** CITATIONS
SEE PROFILE

J|A|C|S
ARTICLES
Published on Web 08/25/2004

Infrared Multiphoton Dissociation Spectroscopy of Gas-Phase Mass-Selected Hydrocarbon−Fe^+ Complexes

Aude Simon,[†,§] William Jones,[†] Jean-Michel Ortega,[‡] Pierre Boissel,[†] Joël Lemaire,[†] and Philippe Maître*,[†]

Contribution from the Laboratoire de Chimie Physique, UMR 8000 du CNRS, Université de Paris-Sud 11, 91405 Orsay CEDEX, France, and Laboratoire pour l'Utilisation du Rayonnement Electromagnétique, UMR 130 du CNRS, Université de Paris-Sud 11, CLIO-BP34, 91405 Orsay CEDEX, France

Received March 2, 2004; E-mail: philippe.maitre@lcp.u-psud.fr

Abstract: Infrared spectra in the mid-infrared region (800−1600 cm^{-1}) of highly unsaturated Fe^+−hydrocarbon complexes isolated in the gas phase are presented. These organometallic complexes were selectively prepared by ion−molecule reactions in a Fourier transform ion cycloton mass spectrometer (FTICR-MS). The infrared multiphoton dissociation (IRMPD) technique has been employed using the free electron laser facility CLIO (Orsay, France) to record the infrared spectra of the mass selected complexes. The experimental IRMPD spectra present the main features of the corresponding IR absorption spectra calculated ab initio. As predicted by these calculations, the experimental spectra of three selectively prepared isomers of Fe^+(butene) present differences in the 800−1100 cm^{-1} range. On the basis of the comparison with calculated IR spectra, the IRMPD spectrum of Fe(butadiene)$^+$ suggests that the ligand presents the s-trans isomeric form. This study further confirms the potentialities of IRMPD spectroscopy for the structural characterization of organometallic ionic highly reactive intermediates in the gas phase. In conjunction with soft ionization techniques such as electrospray, this opens the door to the gas-phase characterization of reactive intermediates associated with condensed phase catalysts.

1. Introduction

The gas-phase reactivity of transition-metal compounds has been extensively studied over the past three decades. Elementary reaction steps mediated by an organometallic ion can be investigated using a large arsenal of mass spectrometric ion−molecule techniques.[1] These mechanistic investigations, restricted until recently to highly unsaturated model compounds, can now be extended to real-world organometallics,[2] which can be smoothly transferred to the gas phase using soft ionization techniques such as electrospray ionization (ESI).[3,4] Catalysis screening, combining in situ syntheses of complexes with ESI, has been achieved to probe the effects of the variation of the metal environnement of Hofmann carbene complexes on olefin metathesis efficiency.[5,6] Several techniques of mass spectrometry can be used, but the Fourier transform ion cyclotron resonance (FTICR)[7] approach is particularly powerful since various methods including ESI can be used to generate ions that can be trapped for a long time, thus allowing combinations of sequences of mass-selections and ion−molecule reactions to specifically generate the molecular ions of interest. High vacuum conditions allow for the trapping of otherwise extremely reactive intermediates, and their reactivity can be studied through ion−molecule reactions by directed collisions between the trapped ionic intermediates with neutral molecules.

Structural characterization of molecular ions is a difficult task. A common way to probe the structures of mass-selected ionic species in an FTICR-MS is to perform, for example, ion−molecule reactions such as H/D exchange reactions, collision-induced dissociation (CID),[8] or photodissociation experiments.[9,10] Nevertheless, all these techniques provide indirect information, and a direct structural characterization such as infrared spectroscopy would be of high interest. IR spectroscopy of molecular ions prepared under FTICR conditions has already been explored,[11−15] but these pioneering studies were limited to the very small tuning range of CO_2 lasers, whose high intensity was required for this particular infrared spectroscopy.

[†] Laboratoire de Chimie Physique.
[‡] Laboratoire pour l'Utilisation du Rayonnement Electromagnétique.
[§] Permanent address: Centre d'Etude Spatiale des Rayonnements, UMR 5187 du CNRS, 9, avenue du Colonel Roche, 31028 Toulouse.

(1) Freiser, B. S. In *Understanding Chemical Reactivity*; Mezey, P. G., Ed.; Kluwer Academic Publisher: Dordrecht, The Netherlands, 1996; Vol. 15.
(2) Plattner, D. A. *Int. J. Mass Spectrom.* **2001**, *207*, 125−144.
(3) Yamashita, M.; Fenn, J. B. *J. Phys. Chem.* **1984**, *88*, 4451.
(4) Yamashita, M.; Fenn, J. B. *J. Phys. Chem.* **1984**, *88*, 4671.
(5) Chen, P. *Angew. Chem., Int. Ed.* **2003**, *42*, 2832−2847.
(6) Volland, M. A. O.; Adlhart, C.; Kiener, C. A.; Chen, P.; Hofman, P. *Chem.−Eur. J.* **2001**, *7*, 4621.
(7) Marshall, A. G.; Hendrickson, C. L.; Jackson, G. S. *Mass Spectrom. Rev.* **1998**, *17*, 1−35.
(8) Rodgers, M. T.; Armentrout, P. B. *Mass Spectrom. Rev.* **2000**, *19*, 215−247.
(9) Dunbar, R. C. *Int. J. Mass Spectrom.* **2000**, *200*, 571−589.
(10) Duncan, M. A. *Int. J. Mass Spectrom.* **2000**, *200*, 545−569.
(11) Hanratty, M. A.; Paulsen, C. M.; Beauchamp, J. L. *J. Am. Chem. Soc.* **1985**, *107*, 5074−5080.
(12) Shin, S. K.; Beauchamp, J. L. *J. Am. Chem. Soc.* **1990**, *112*, 2057−2066.
(13) Shin, S. K.; Beauchamp, J. L. *J. Am. Chem. Soc.* **1990**, *112*, 2066−2069.
(14) Ranasinghe, Y. A.; Surjasasmita, I. B.; Freiser, B. S. In *Understanding Chemical Reactivity*; Freiser, B. S., Ed.; Kluwer Academic Publisher: Dordrecht, The Netherlands, 1996; Vol. 15; pp 229−258.
(15) Surya, P. I.; Roth, L. M.; Ranatunga, D. R. A.; Freiser, B. S. *J. Am. Chem. Soc.* **1996**, *118*, 1118−1125.

10.1021/ja0488176 CCC: $27.50

Indeed, traditional IR absorption techniques cannot be used for IR spectroscopy of isolated gas-phase ionic complexes because of the inherent problem of low ion density. However, providing the use of an intense IR source, one can induce fragmentation of the ion of interest, the dissociation threshold being reached after the absorption of several IR photons. The IR multiphoton dissociation (IRMPD) process can then easily be probed with great sensitivity using mass spectrometry.

IR free-electron lasers (FELs) such as CLIO[16,17] or FELIX[18] are particularly suitable for this particular IR spectroscopy of molecular ions since they provide both high brightness and tunability over a wavelength range covering the so-called infrared molecular fingerprint. Their large tuning range (110−3000 cm^{-1} at CLIO) is an advantage for IR spectroscopy of ionic gas-phase species over modern optic parametric oscillators (OPO), which do not cover the wavelengths below 2000 cm^{-1} with high enough intensity.[19−21] IR spectroscopy using the IRMPD induced by the IR−FEL has been undertaken for a large variety of ions, including polycyclic aromatic hydrocarbons (PAH),[22−24] clusters,[25] and metal−benzene complexes.[26] A coupling of a tunable IR−FEL to an FTICR-MS instrument has been realized at CLIO,[27] allowing for the selective preparation of an ion. Using this experimental setup, IRMPD spectra of organometallic species,[27−31] organic cations,[32] as well as sodiated amino acid complexes[33] and protonated dipeptides[34] have been recorded. The attachment site of Cr^+ to gas-phase aniline[35] has also recently been probed by IRMPD spectroscopy using an experimental setup combining FTICR-MS and IR−FEL at FELIX.

The primary motivation for studying the present complexes is to show the potential of IRMPD spectroscopy for characterizing organometallic reactive intermediates involved in the hydrocarbon activation by third-row transition-metal cations M^+ in the gas phase.[36,37] As shown in the pioneering work of Irikura and Beauchamp, a sequence of several methane activation steps is observed when M^+ is allowed to react with methane in FTICR conditions.[38] In the case of M = Ta and W in particular, four successive methane dehydrogenations are observed as evidenced by the observation of $MC_nH_{2n}^+$ ($n = 1-4$). The $FeC_4H_8^+$ isomers studied in this work have been chosen because they present the same stoichiometry as the last reactive intermediate ($MC_4H_8^+$) of this sequence. The structures of the $FeC_4H_8^+$ complexes, generated under FTICR conditions, have been investigated by Freiser and co-workers by different means, including IRMPD using a cw CO_2 laser.[15] The use of a FEL laser in the present work offering a continuous tuning over a large wavelength range is thus also interesting to provide a complete molecular fingerprint of these Fe^+ complexes. Data corresponding to one of these Fe^+ complexes have been used to illustrate the potentialities of the experimental setup,[28] and we herein present and discuss the IR spectra of three isomers of Fe^+(butene) along with the IR spectrum of Fe^+(butadiene).

2. Methods

2.1. Coupling Free-Electron Laser CLIO and FTICR-MS MICRA. The experimental setup has been described in detail previously.[27] On the basis of a 1.24 T permanent magnet, made of an assemblage of two Halbach cylinders,[39] MICRA[40] is an easily transportable FTICR mass spectrometer. The main vacuum chamber was pumped with a 70 L/s turbomolecular pump, backed with a three-stage diaphragm pump, allowing for a background pressure of about 3×10^{-9} Torr. The ICR cell was cubic-like ($2 \times 2 \times 2$ cm^3), where the two excitation electrodes were replaced by sets of four interconnected electrodes to provide optical access to the IR−FEL through a ZnSe entrance window.

Primary ions were generated in the ICR cell. Laser ablation[29,37] or MALDI[33,34] could now be used, but in the present case, electron impact (EI) at ca. 70 eV on neutral $Fe(CO)_5$ pulsed with a pressure of 10^{-6} Torr was used. Two types of reaction sequences[15] were used to produce $FeC_4H_8^+$ ions in three different ways (eq 1). $FeC_4H_8^+$ ions were generated by dehydrogenation of isobutane by mass-selected Fe^+ (eq 1a), presumably leading exclusively to Fe^+(i-butene). $FeC_4H_8^+$ ions were also generated by ligand displacement of CO from mass-selected $FeCO^+$ by 2-butene (eq 1b) and 1-butene (eq 1c). Typically, after the mass selection of Fe^+ or $FeCO^+$ from $Fe(CO)_n^+$ ($n = 0-5$), ions produced by EI, Fe^+, or $FeCO^+$ were allowed to react with neutral gas pulsed during 50 and 100 ms, respectively, before mass selection of $FeC_4H_8^+$ ions, and their irradiation for typically 500 ms.

$$Fe^+ + \text{i-butane} \rightarrow FeC_4H_8^+ + H_2 \rightarrow \text{mass selection} \rightarrow FeC_4H_8^+ \quad (1a)$$

$$FeCO^+ + \text{2-butene} \rightarrow FeC_4H_8^+ + CO \rightarrow \text{mass selection} \rightarrow FeC_4H_8^+ \quad (1b)$$

$$FeCO^+ + \text{1-butene} \rightarrow FeC_4H_8^+ + CO \rightarrow \text{mass selection} \rightarrow FeC_4H_8^+ \quad (1c)$$

As mentioned in the Introduction, IR−FEL[16−18] has been shown to provide the required characteristics to perform IRMPD spectroscopy:

(16) Jaroszynski, D. A.; Prazeres, R.; Glotin, F.; Ortega, J. M. *Phys. Rev. Lett.* **1994**, *72*, 2387−2390.
(17) Prazeres, R.; Glotin, F.; Insa, C.; Jaroszynski, D. A.; Ortega, J. M. *Eur. Phys. J. D* **1998**, *3*, 87−93.
(18) Oepts, D.; van der Meer, A. F. G.; Amersfoot, P. W. *Infrared Phys. Technol.* **1995**, *36*, 297−308.
(19) Dopfer, O.; Olkhov, R. V.; Roth, R. V.; Maier, J. P. *Chem. Phys. Lett.* **1998**, *296*, 585.
(20) Grégoire, G.; Velasquez, J.; Duncan, M. A. *Chem. Phys. Lett.* **2001**, *2001*, 451.
(21) Robertson, W. H.; Price, E. A.; Weber, J. M.; Shin, J. W.; Weddle, G. H.; Johnson, M. A. *J. Phys. Chem.* **2003**, *2003*, 6527.
(22) Oomens, J.; van Roij, A. J. A.; Meijer, G.; von Helden, G. *Astrophys. J.* **2000**, *542*, 404−410.
(23) Oomens, J.; Meijer, G.; von Helden, G. *J. Phys. Chem. A* **2001**, *105*, 8302−8309.
(24) Oomens, J.; Sartakov, B. G.; Tielens, A.; Meijer, G.; von Helden, G. *Astrophys. J.* **2001**, *560*, *Part 2*, L99−L103.
(25) van Heijnsbergen, D.; Duncan, M. A.; Meijer, G.; von Helden, G. *Chem. Phys. Lett.* **2001**, *349*, 220−226.
(26) van Heijnsbergen, D.; von Helden, G.; Meijer, G.; Maître, P.; Duncan, M. A. *J. Am. Chem. Soc.* **2002**, *124*, 1562−1563.
(27) Maitre, P.; Le Caer, S.; Simon, A.; Jones, W.; Lemaire, J.; Mestdagh, H.; Heninger, M.; Mauclaire, G.; Boissel, P.; Prazeres, R.; Glotin, F.; Ortega, J. M. *Nucl. Instrum. Methods, Sect. A* **2003**, *507*, 541−546.
(28) Lemaire, J.; Boissel, P.; Heninger, M.; Bellec, G.; Mestdagh, H.; Simon, A.; Le Caer, S.; Ortega, J. M.; Glotin, F.; Maitre, P. *Phys. Rev. Lett.* **2002**, *89*, 273002/1−273002/4.
(29) Reinhard, B. M.; Lagutschenkov, A.; Lemaire, J.; Boissel, P.; Maitre, P.; Niedner-Schatterburg, G. *J. Phys. Chem.* **2004**, *108*, 3350−3355.
(30) Le Caer, S.; Lemaire, J.; Maitre, P.; Mestdagh, H. *Chem. Phys. Lett.* **2004**, *385*, 273−279.
(31) MacAleese, L.; Simon, A.; Lemaire, J.; Boissel, P.; Maitre, P. To be submitted for publication.
(32) Jones, W.; Boissel, P.; Chiavarino, B.; Crestoni, M. E.; Fornarini, S.; Lemaire, J.; Maitre, P. *Angew. Chem., Int. Ed.* **2003**, *42*, 2057−2059.
(33) Kapota, C.; Lemaire, J.; Maitre, P.; Ohanessian, G. *J. Am. Chem. Soc.* **2004**, *126*, 1836−1842.
(34) Lucas, B.; Grégoire, G.; Lemaire, J.; Maître, P.; Ortega, J. M.; Rupenyan, A.; Reimann, B.; Schermann, J. P.; Desfrançois, C. *Phys. Chem. Chem. Phys.* **2004**, *6*, 2659−2663.
(35) Oomens, J.; Moore, D. T.; von Helden, G.; Meijer, G.; Dunbar, R. C. *J. Am. Chem. Soc.* **2004**, *126*, 724−725.
(36) Simon, A.; Lemaire, J.; Boissel, P.; Maître, P. *J. Chem. Phys.* **2001**, *115*, 2510.
(37) Simon, A.; MacAleese, L.; Boissel, P.; Lemaire, J.; Maître, P. To be submitted for publication.
(38) Irikura, K. K.; Beauchamp, J. L. *J. Phys. Chem.* **1991**, *95*, 8344−8351.
(39) Coey, J. M. D. *J. Magn. Magn. Mater.* **2002**, *248*, 441−456 (Pt 2).
(40) Mauclaire, G.; Lemaire, J.; Boissel, P.; Bellec, G.; Heninger, M. *Eur. J. Mass Spectrom.* **2004**, *1*, 155−162.

high peak power, relatively small bandwidth, and easy tunability in the mid-infrared region. These characteristics could be found at the CLIO infrared FEL facility.[16,17] The IR−FEL CLIO[16,17] at Orsay provided a very large wavelength range in the infrared (from 3 to 90 μm). For a given electron energy between 10 and 50 MeV, continuous tunability was obtained over a spectral range of $\Delta\lambda/\lambda \cong 2.5$. In the present case, the whole fingerprint spectral range (800−1600 cm^{-1}) was covered with a single electron energy (40 MeV). Overall, the FEL relative bandwidth (fwhm) was about 0.3−0.5%. The FEL output consisted of 8-μs-long macropulses fired at a repetition rate of 25 Hz. Each macropulse contained 500 micropulses, each a few picoseconds long. The mean IR power was about 500 mW, corresponding to micropulse and macropulse energies of 40 μJ and 20 mJ, respectively, and to a peak power of ca. 20 MW.

The IR−FEL beam, perpendicular to the magnetic field, was focused in the ICR cell with a 1-m focal length spherical mirror. The focalization distance was tuned so as to optimize the IRMPD yield at about 5 μm for $Fe(CO)_5^+$. At this IR wavelength, the laser beam waist was estimated to be 200 μm, which was likely to be smaller than the ion cloud. Nevertheless, providing an irradiation time of 500 ms, total photofragmentation of $Fe(CO)_5^+$ was observed, indicating that all ions eventually interacted with the IR beam. The irradiation time was set by a fast electromechanical shutter, synchronized with the FEL, that allowed for the selection of a given number of macropulses.

The IR−FEL wavelength was scanned by steps of 6 cm^{-1}, close to the FEL bandwidth. For each wavelength, a mass spectrum was derived from an ion signal accumulated over 10 sequences and the IRMPD rate R could be defined as $R = -\log[I_{parent}/(I_{parent} + \Sigma I_{fragment})]$. As a matter of fact, preliminary measurements showed that the normalized parent ion intensity decayed exponentially with the number N of macropulses. This showed that, during each macropulse, a nearly constant fraction $r = R/N$ of parent ions was dissociated.

In the present case, because the IRMPD rate dependence over intensity was not precisely known, we preferred to give the raw data. Indeed, this dependence should be an *S*-shaped curve, exhibiting a threshold behavior at low intensity because of the nonlinear nature of the IRMPD process and a saturation at high intensity. Under our experimental conditions, the rate variation with intensity was often close to linear, as was observed for the dissociation of $Fe(CO)_5$.[28] At lower intensity the rate decreased faster, consistent with the power of two law observed in experiments at FELIX.[22] If a correction was applied, it should also take into account the variation of the laser fluence as a function of the wavelength. Indeed, assuming a diffraction limited beam, the waist area should be 4 times larger at 800 cm^{-1} than at 1600 cm^{-1}. However, the ion cloud being not located exactly at the waist, the area variation should not be larger than a factor of 2.

2.2. Vibrational Calculations. Vibrational frequency calculations of $FeC_4H_8^+$ isomers were performed with Gaussian 98 package[41] using the hybrid B3LYP functional. The metal was represented by a [8s6p4d1f]/(14s11p6d3f) basis set,[42] and a polarized double-ζ quality basis set[43] was used for the ligands. B3LYP was chosen for two reasons. First, early on it was shown to provide a good description of the energetics of transition metal-containing systems.[44,45] Furthermore, providing the use of an appropriate scaling, hybrid DFT methods such as B3LYP were shown to outperform other DFT as well as traditional ab initio approaches to describe both the positions[46] and the relative intensities[47] of IR bands.

Considering the wavelength range (800−1600 cm^{-1}) explored in the present work, the probed vibrations of the Fe^+(butene) complexes should be the ones of the free alkene ligand[48] shifted because of the interaction with the metal cation, the three metal−ligand vibrations being lower in energy (300−500 cm^{-1}). The scaling factor was known to strongly depend on the method but also on the vibrational wavelength range, and this factor should be larger for the stretching modes than for the other ones.[46] A scaling factor was derived for the vibrations of interest in the present work using the positions of the most intense IR bands of isobutene and ethylene.[48] This led to a value of 0.98 for the scaling factor, the absolute average difference between the two spectra being 10 cm^{-1}. This scaling factor was also used to derive the differences between the zero-point energies, and thus the enthalpies at 0 K of all the calculated isomers are given below.

3. Results

The IRMPD yield of $FeC_4H_8^+$ ions has been recorded as a function of IR wavelength ranging from 800 through 1600 cm^{-1}. When $FeC_4H_8^+$ ions are obtained through dehydrogenation of i-butane as in eq 1a, only the Fe^+ photofragment is observed, whereas when ligand exchange reactions (eq 1b,c) are used to produce $FeC_4H_8^+$ ions, two photofragments ($FeC_4H_6^+$ and Fe^+) are observed. These observations are consistent with those of Freiser and co-workers[15] and support that $FeC_4H_8^+$ ions formed through dehydrogenation reaction (eq 1a) correspond to Fe^+-(i-butene), and one can expect that no isomerization occurs during the ligand exchange reactions (eq 1b,c).

The experimental IRMPD spectra of the mass-selected $FeC_4H_8^+$ ions prepared as in reactions eq 1a−c are given in Figure 1 and compared to the calculated IR spectra of the Fe^+ complexes of i-butene, 2-*E*-butene, and 1-butene. Overall, there is a good agreement between the IRMPD rates (solid line) and the corresponding calculated absorption spectra (stick bars) for the three Fe^+ complexes. The calculated positions and intensities of the vibrational IR active bands of these three complexes are given in Table 1, along with those of the free ligands.

These calculated IR spectra are associated with the lowest-energy structures of the Fe^+ complexes of i-butene, 1-butene, and 2-*E*-butene given in Figure 2. All the minimum energy structures given in Figure 2 correspond to a quartet spin state correlating to the $Fe^+[^4F(d^7)]$+butene excited asymptote, 5.8 kcal/mol[49] higher than the $Fe^+[^6D(sd^6)]$+butene ground-state asymptote. This spin-crossing, already found by Bauschlicher and co-workers in the case of Fe^+(ethylene),[50] is due to the fact that the d^7 electronic configuration on Fe^+ allows for a closer approach of the ligand and thus increases the electrostatic and charge-transfer components of the Fe^+−alkene interaction. The lowest-energy structure found for all the present complexes correspond to an electronic configuration where the 3d orbital that overlaps with the π*-orbital of the alkene is doubly occupied, so as to maximize the metal-to-ligand back-donation.

(41) Frisch, M. J.; Trucks, G. W.; Schlegel, H. B.; Scuseria, G. E.; Robb, M. A.; Cheeseman, J. R.; Zakrzewski, V. G.; Montgomery, J. A., Jr.; Stratmann, R. E.; Burant, J. C.; Dapprich, S.; Millam, J. M.; Daniels, A. D.; Kudin, K. N.; Strain, M. C.; Farkas, O.; Tomasi, J.; Barone, V.; Cossi, M.; Cammi, R.; Mennucci, B.; Pomelli, C.; Adamo, C.; Clifford, S.; Ochterski, J.; Petersson, G. A.; Ayala, P. Y.; Cui, Q.; Morokuma, K.; Malick, D. K.; Rabuck, A. D.; Raghavachari, K.; Foresman, J. B.; Cioslowski, J.; Ortiz, J. V.; Stefanov, B. B.; Liu, G.; Liashenko, A.; Piskorz, P.; Komaromi, I.; Gomperts, R.; Martin, R. L.; Fox, D. J.; Keith, T.; Al-Laham, M. A.; Peng, C. Y.; Nanayakkara, A.; Gonzalez, C.; Challacombe, M.; Gill, P. M. W.; Johnson, B. G.; Chen, W.; Wong, M. W.; Andres, J. L.; Head-Gordon, M.; Replogle, E. S.; Pople, J. A. *Gaussian 98*, revision A.6; Gaussian, Inc.: Pittsburgh, PA, 1998.
(42) Bauschlicher, C. W., Jr. *Theor. Chim. Acta* **1995**, *92*, 183−198.
(43) Hay, P. J. *J. Chem. Phys.* **1977**, *66*, 4377−4384.
(44) Bauschlicher, C. W.; Maître, P. *J. Phys. Chem.* **1995**, *99*, 3444.
(45) Maître, P.; Bauschlicher, C. W., Jr. *J. Phys. Chem.* **1995**, *99*, 6836.
(46) Halls, M. D.; Velkovski, J.; Schlegel, H. B. *Theor. Chim. Acc.* **2001**, *105*, 413.
(47) Halls, M. D.; Schlegel, H. B. *J. Chem. Phys.* **1998**, *109*, 10587−10593.
(48) Jacox, M. E. NIST Standard Reference Database Number 69, March 2003. NIST Chemistry WebBook Home Page. http://webbook.nist.gov/chemistry/.
(49) *Atomic Energy Levels*; Moore, C. E., Ed.; U.S. Department of Commerce, National Bureau of Standards: Washington, DC, 1971; Vol. II.
(50) Sodupe, M.; Bauschlicher, C. W.; Langhoff, S. R.; Partridge, H. *J. Phys. Chem.* **1992**, *96*, 2118−2122.

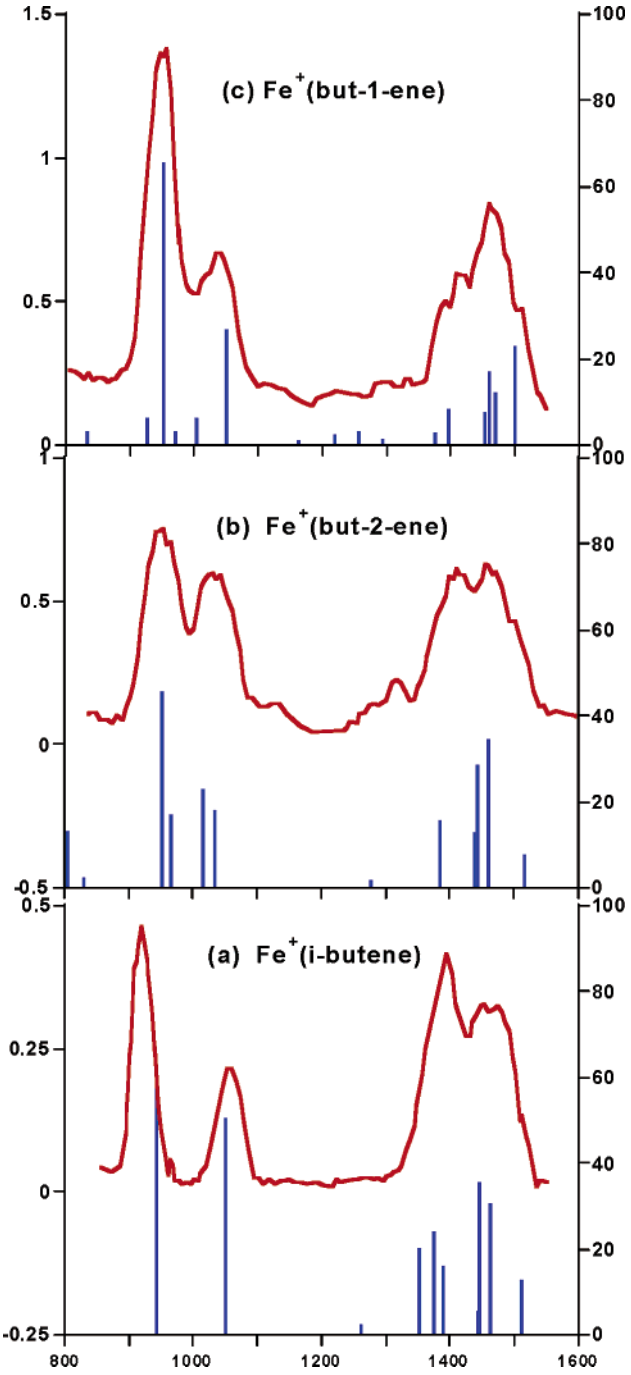

Figure 1. IRMPD spectrum and calculated IR absorption spectrum (blue stick bars) of Fe(i-butene)$^+$ (a), Fe(2-butene)$^+$ (b), and Fe(1-butene)$^+$ (c). IRMPD yields (red line) are expressed as the neperian logarithm of the normalized fragment intensity $R = -\log[I_{parent}/(I_{parent} + \Sigma I_{fragment})]$. Calculated intensities (right scale) are given in km/mol.

As a result, a substantial lengthening (+0.06 Å) of the C═C bond in the Fe^+ complex (Figure 2) as compared to that of the free ligand was calculated for the three complexes, in good agreement with the calculated values in the case of the $Fe^+(C_2H_4)$ complex.[50]

4. Discussion

4.1. IRMPD versus IR Spectra. IRMPD has already been shown to provide a powerful tool to derive infrared spectra of mass-selected molecular ions. Indeed, despite the multiple photon character of the IRMPD process, it seems that with the IR fluence provided by the FEL, no fragmentation occurs unless the first photon is resonant with a fundamental vibrational state of the parent ion. The absorption of the subsequent photons is believed to proceed via two successive regimes,[51,52] the transition between these two processes depending on the density of vibrational states and the coupling between the resonant state and the vibrational bath. The absorption of the first photons occurs within the discrete regime, in which a particular vibration is excited resonantly. Subsequent excitations occur within the quasi-continuum regime in which the density of states is so high that the vibrational energy is rapidly statistically randomized[53] among all the vibrational modes of the ion. The absorption of the first few photons within the discrete regime[51,52] is generally believed to govern the relative intensities of the IRMPD spectrum and might be at the origin of the good agreement between the IRMPD and linear absorption spectra.

In the present case, a satisfactory agreement has been found between the relative intensities of the IRMPD spectra and the ones of the calculated linear absorption spectra. It should also be noted that the present ions are relatively small, and thus, larger deviations from the linear absorption intensities over the spectral range might occur if several photons are required to reach the quasi-continuum regime.

The main purpose of this work was to probe the performance of IR spectroscopy to distinguish between three isomers of Fe^+(butene). As can be seen in Figure 1, in good agreement with the calculated spectra, the three recorded IRMPD spectra display two main features, one at low energy (800−1100 cm^{-1}) and the other between 1350 and 1550 cm^{-1}. The IRMPD spectrum of $FeC_4H_8^+$ ions generated by eq 1a is given in Figure 1a. As mentioned earlier, the fragmentation patterns of the corresponding ions suggest that they correspond to Fe^+(i-butene) complexes and, as predicted by theory, the IRMPD spectrum of Fe^+(i-butene) is clearly different from the two others, especially in the low-energy range featuring two bands with maxima at 920 and 1060 cm^{-1}. The IRMPD maximum at 920 cm^{-1} should owe its origin to the ethylenic CH_2 wagging mode predicted at 942 cm^{-1}. At 1051 cm^{-1}, a combination of out-of-plane CH_3 rocking modes is also predicted to be very intense (Table 1) and should correspond to the IRMPD maximum observed at 1060 cm^{-1}. The low-energy region of the IRMPD spectrum of the Fe^+(i-butene) is also interesting for providing an extent of the intrinsic broadening of each IR transition within the experimental conditions. Indeed, the two predicted IR active bands are clearly separated so that one can assume that the IRMPD band observed at 920 (1060) cm^{-1} is the result of the IR absorption through the calculated band at 942 (1051) cm^{-1}. The fwhm of these two IRMPD bands, which is about 50 cm^{-1}, is very similar to the IRMPD bandwidth observed in the case of $Fe^+(CH_3OCH_3)_2$, which also exhibits five well-separated IR active bands.[27,30] It seems, therefore, that the IRMPD bandwidth is much larger than the fwhm of the IR−FEL, which is about 5 cm^{-1} in this wavelength range.

The high-energy part of the IRMPD spectrum of Fe^+-(i-butene), between 1350 and 1550 cm^{-1} (Figure 1a), presents a broad band with two maxima (1400 and 1450−1470 cm^{-1}). These two overlapping bands can be assigned on the basis of

(51) Mukamel, S.; Jortner, J. *J. Chem. Phys.* **1976**, *65*, 5204−5225.
(52) Lee, Y. T. *J. Chem. Phys.* **1979**, *70*, 912−929.
(53) Black, J.; Tablonovitch, E.; Bloembergen, N.; Mukamel, S. *Phys. Rev. Lett.* **1977**, *38*, 1131.

Table 1. Description of the Vibrational Modes of the Fe^+(i-butene), Fe^+(2-butene), and Fe^+(1-butene) Complexes[a]

1-butene		2-butene		i-butene		
complex	*free*	complex	*free*	complex	*free*	mode description
1499 (23)	***1669 (15)***	**1518 (7)**	***1701 (0)***	**1510 (12)**	***1685 (27)***	C═C stretch
1470 (12)	***1474 (9)***	**1459 (34)**	***1464 (24)***	**1462 (31)**	***1471 (16)***	CH_3 d-deform
1459 (17)	***1463 (8)***	**1444 (28)**	***1456 (0)***	**1446 (35)**	***1456 (24)***	CH_3 d-deform
		1441 (13)	***1448 (0)***	1443 (5)	*1450 (5)*	CH_3 d-deform
		1440 (1)	*1447 (20)*	1430 (1)	*1440 (0)*	CH_3 d-deform
1454 (7)	***1450 (6)***					$CH_2(C_2H_5)$ wagging
1396 (8)	*1421 (3)*					CH IP (scis)
1376 (3)	*1378 (4)*	**1387 (15)**	***1383 (8)***	**1389 (16)**	***1381 (1)***	CH_3 s-deform
		1386 (0)	*1384 (0)*	**1376 (24)**	***1382 (19)***	CH_3 s-deform
1294 (1)	*1310 (2)*					$CH_2(C_2H_5)$ twist
1258 (3)	*1254 (0)*					$CH_2(C_2H_5)$ rock
1218 (2)	*1279 (1)*	1279 (1)	*1292 (3)*			CH IP (scis)
		1236 (0)	*1295 (0)*	**1352 (20)**	***1415 (3)***	CH IP (scis)
		1132 (0)	*1139 (0)*			CH_3 rock
		1034 (7)	*1037 (0)*			CH_3 rock
1163 (1)	*1171 (0)*	**1033 (18)**	***1056 (2)***	1260 (2)	*1274 (5)*	C−C stretch
1051 (27)	***1066 (5)***					$CH_2(C_2H_5)$ (scis)
				1051 (50)	***1075 (3)***	CH_3 rock
		1015 (23)	***1036 (0)***	1032 (0)	*1051 (6)*	CH_3 rock
				984 (0)	*992 (0)*	CH_3 rock
				947 (0)	*936 (0)*	CH_3 rock
1005 (6)	*999 (12)*	**966 (17)**	***977 (53)***	**942 (57)**	***914 (69)***	CH OOP (wag)
972 (3)	*1010 (4)*	**954 (45)**	***960 (21)***			CH_3 rock
953 (65)	***922 (65)***					CH OOP (wag)
927 (6)	*961 (6)*			910 (0)	*965 (0)*	CH IP (rock)
834 (3)	*842 (3)*	831 (2)	*856 (0)*	769 (4)	*799 (0)*	C−C stretch
783 (6)	*774 (5)*					CH_3 rock
706 (5)	*631 (12)*	805 (13)	*731 (0)*	732 (5)	*685 (0)*	CH OOP (twist)

[a] Calculated vibrational wavenumbers are given in cm^{-1} and corresponding intensities (in parentheses) are given in km/mol. The values in italics correspond to the free ligands. The most intense vibrational modes are given in bold.

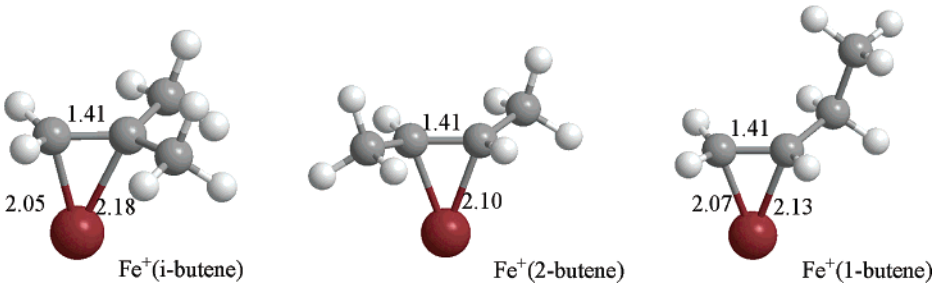

Figure 2. Structures of the lowest-energy quartet spin states of Fe(i-butene)$^+$, Fe(1-butene)$^+$, and Fe(2-butene)$^+$. Distances are given in angstroms.

the calculated spectrum of Fe^+(i-butene), and their broadening character can be explained by the fact that each IRMPD band might be the result of initial absorption through three closely spaced IR absorption bands. The IRMPD maximum at 1400 cm^{-1} can be assigned to two combinations of the symmetric CH_3 deformation (1376 and 1389 cm^{-1}) and the CH_2 scissoring (1352 cm^{-1}). The broad band in the IRMPD spectrum with a maximum at 1450−1470 cm^{-1} should owe its origin to three other vibrational modes that are also predicted to be intense: two combinations of disymmetric CH_3 deformations (1446 and 1462 cm^{-1}), which are separated from the ethylenic C═C stretch at 1510 cm^{-1}.

Upon complexation to Fe^+, there is a shift of the IR bands of the ligand and, to facilitate the discussion, the IRMPD spectrum of Fe^+(i-butene) and the gas-phase IR spectrum[48] of the free i-butene are displayed in Figure 3, and they can be compared to the calculated IR bands (stick bars in Figure 3). As can be seen in Figure 3, the C═C stretch mode is significantly red-shifted (by −174 cm^{-1}) upon complexation: this vibrational mode is predicted at 1685 cm^{-1} in the free ligand and at 1511 cm^{-1} in Fe^+(i-butene). Whereas it is about 200 cm^{-1} higher in energy than the CH_3 deformations modes in the free ligand, the red shift associated to the complexation brings it very close to these modes in the complex (Figure 3). Another vibrational mode of the alkene is significantly red-shifted upon complexation. This is the CH_2 scissoring mode, calculated at 1352 cm^{-1} in the case of Fe^+(i-butene), thus corresponding to a red shift of −63 cm^{-1} upon complexation. On the contrary, the CH_2 wagging mode calculated at 942 cm^{-1} is blue-shifted (+27 cm^{-1}) upon complexation. Finally, it is interesting to compare the relative broadening of the IRMPD bands (Figure 3a) with the one associated to the one photon IR spectroscopy of the gas-phase ligand (Figure 3b). The resolution of the IR light source used for i-butene is about 4 cm^{-1}, and it is thus similar to the bandwidth (fwhm) of the IR−FEL in the wavelength range. Overall, the band shape of the IRMPD spectrum of Fe^+−i-butene is very similar to the one of the IR spectrum of gas-phase i-butene taken at room temperature. If one considers, for instance, the C═C vibrational mode of i-butene at 1685 cm^{-1}, the fwhm of the associated IR band is about 50 cm^{-1}. That is, it is of the same order of magnitude as the fwhm of the IRMPD bands observed through IRMPD for

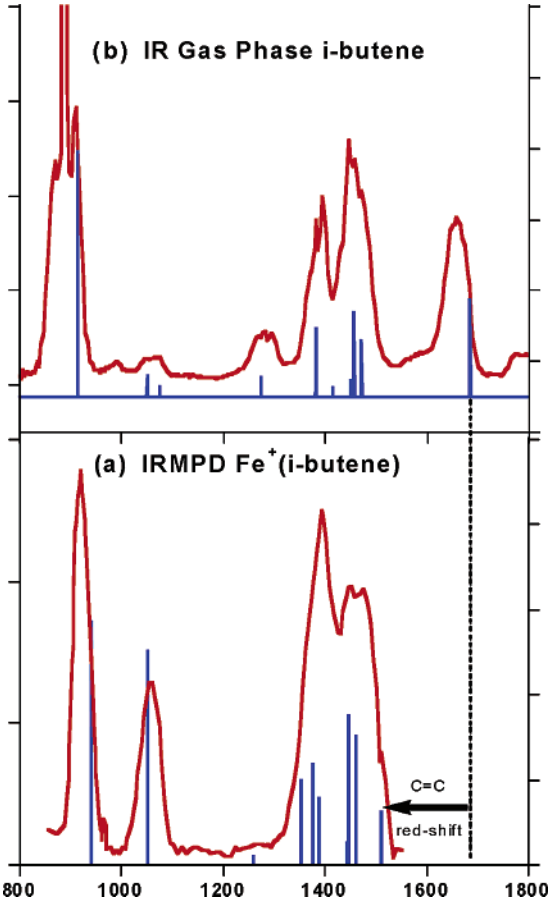

Figure 3. IRMPD spectrum and calculated IR absorption spectrum (stick bars) of Fe(i-butene)$^+$ (a). IR spectrum of gas-phase i-butene and its calculated IR absorption spectrum (stick bars) (b). Calculated intensities (right scale) are given in km/mol.

the molecular ions under FTICR-MS conditions.[27,30] One may thus consider that the IRMPD band shape of molecular ions is affected by the multiphotonic character of the IRMPD process, but the comparison above suggests that the IRMPD band shape is mainly due to the rotational bandwidth of the molecular ions at room temperature.

The IRMPD spectrum of $FeC_4H_8^+$ ions produced as in eq 1b is given in Figure 1b. As for the ions generated by dehydrogenation of i-butane (eq 1a), two bands are observed in the lower-energy part of the spectrum (800−1100 cm^{-1}). Nevertheless, these two bands are closer to each other in Figure 1b (950 and 1020−1040 cm^{-1}) than in Figure 1a (920 and 1060 cm^{-1}), and the bandwidth is larger in the former than in the later case. Both of these observations suggest that $FeC_4H_8^+$ ions generated as in eq 1b are different from the ones obtained by eq 1a and correspond to Fe^+(2-butene) complexes. The IRMPD band at 950 cm^{-1} in Figure 1b can be assigned to the contribution of two calculated IR bands of Fe^+(2-butene), the most intense corresponding to CH_3 rocking mode (954 cm^{-1}), the other to an out-of-plane ethylenic CH bending (966 cm^{-1}). Similarly, the second IRMPD band with a maximum at 1020−1040 cm^{-1} can be assigned to two bands: a CH_3 rocking mode at 1015 cm^{-1} and the symmetric combination of the C−C stretches at 1033 cm^{-1}. The fact that the absorption of the first IR photon might proceed through two different modes might explain the broadening observed in Figure 1b. One could also think that the fact the two calculated bands at 1015 and 1033 cm^{-1} present similar intensities could be at the origin of the larger maximum observed at 1020−1040 cm^{-1} than at 950 cm^{-1} in Figure 1b, the first steps of the IRMPD process in the latter case being more favorable when the IR laser is in resonance with the most intense IR absorption band calculated at 954 cm^{-1}. Finally, the positions of the most intense IR absorption bands in the calculated IR absorption spectra of Fe^+(2-butene) and Fe^+(i-butene) nicely explain the observation of an overlap between the two IRMPD bands in Figure 1b while they are clearly separated in Figure 1a.

The upper part of the IRMPD spectrum given in Figure 1b essentially consists of a broad band where one can distinguish two maxima at 1410 and 1460 cm^{-1}. This band could be assigned to several vibrational modes of Fe^+(2-butene) (Table 1), corresponding to disymmetric deformation of CH_3 groups (the most intense at 1441, 1444, and 1459 cm^{-1}). As in the case of Fe^+(i-butene), the C═C stretching mode is predicted to be significantly red-shifted in the complex (1518 cm^{-1}) as compared to that of the free ligand (1701 cm^{-1}), and it should therefore contribute to the absorption on the blue side of the broad IRMPD band. A small IRMPD band is also observed at 1320 cm^{-1}, which can be tentatively assigned to a symmetric deformation mode of the methyl groups calculated at 1387 cm^{-1}.

The IRMPD spectrum of $FeC_4H_8^+$ ions produced as in eq 1c is given in Figure 1c, where it can be compared to the calculated IR absorption spectrum of Fe^+(1-butene). The corresponding data have already been discussed extensively.[28] The two overlapping bands observed in the lower-energy part of the IRMPD spectrum, with maxima at 950 and 1035 cm^{-1}, can be assigned to the two most intense IR modes in this region, the ethylenic wagging (953 cm^{-1}) and the CH_2 scissoring of the ethyl group (1051 cm^{-1}), respectively. The IRMPD spectrum in Figure 1c differs from the one in Figure 1b by the relative intensities of the two bands in the low-energy part of the spectrum and also by the broadening of the lowest-energy band. As discussed above, the broadening of the band at 950 cm^{-1} in Figure 1b occurs because the IRMPD process can initiate through a photon absorption in two different modes, while absorption through the wagging mode should dominate in the case of Fe^+(1-butene), leading to the band at 950 cm^{-1} in Figure 1c.

At higher energy, the IRMPD spectrum in Figure 1c displays a broad band with a single maximum at 1460 cm^{-1} and a double shoulder (1390 and 1416 cm^{-1}) on its red side. These features are in very good agreement with the theoretical IR spectrum of Fe^+(1-butene). As in the other two cases, the C═C stretch (1499 cm^{-1} in Table 1) is significantly red-shifted (−170 cm^{-1}) as compared to the free ligand. Absorption through this vibrational mode should thus contribute to the blue side of the IRMPD band, as in the case of the other two isomers. Going toward the lowest energies, two vibrational modes corresponding to deformations of C_2H_5 (1454, 1459, and 1470 cm^{-1}, see Table 1) are expected to play a role in the IRMPD process. A band calculated at 1396 cm^{-1} and corresponding to in-plane CH bending could explain the shoulder observed on the red side of maximum of the IRMPD spectrum in this region.

4.2. Photodissociation Features. Overall, the IRMPD yield in the case Fe(i-butene)$^+$ is smaller than in the case of its two isomers Fe(1-butene)$^+$ and Fe(2-butene)$^+$. This difference might be because the dissociation threshold is much larger in the first

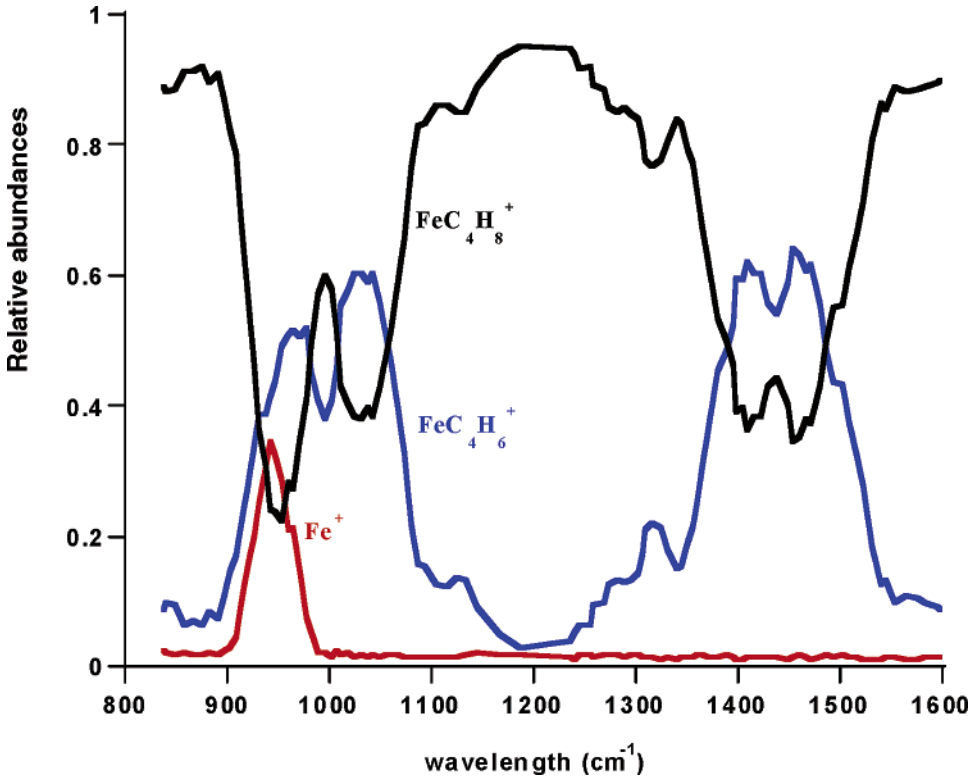

Figure 4. Parent $FeC_4H_8^+$ and fragments (Fe^+, $FeC_4H_6^+$) relative intensities as a function of the wavelength observed for the IRMPD of $FeC_4H_8^+$ ions produced by ligand exchange reaction $FeCO^+$+2-butene.

than in the two latter cases. Indeed, in the case of the Fe(i-butene)$^+$ complex, the only ion fragment observed is Fe^+, and the fragmentation corresponds to the loss of the whole i-butene ligand. In the case of Fe(1-butene)$^+$ and Fe(2-butene)$^+$ isomers, however, the main photofragment is $FeC_4H_6^+$, presumably corresponding to Fe(butadiene)$^+$.[15] This ion is generated by the loss of H_2, which is energetically less demanding than the loss of the whole butene ligand. Therefore, one can expect that the dissociation of Fe(i-butene)$^+$ requires a larger number of IR photons than the one of its two isomers, and this is probably at the origin of the difference in the observed IRMPD yields.

The fragmentation patterns of these Fe(butene)$^+$ isomers, along with others such as $Fe(C_2H_4)_2^+$, have been studied by Freiser and co-workers[15] under FTICR-MS conditions using a combination of techniques, including IRMPD with a CO_2 laser that is at a fixed wavelength 10.6 μm (944 cm^{-1}). Two other approaches were used, including CID and sustained off-resonance irradiation (SORI). This latter method can be considered as mimicking the IR multiphoton photon energization process since it provides a slow increase of the internal energy of the parent ion through collisions induced by multiple acceleration−deceleration cycles,[54] and as a matter of fact, SORI and IRMPD results at 944 cm^{-1} were very similar.[15] Fe(butene)$^+$ complexes were generated through ligand exchange or dehydrogenation in eq 1a−c as in the present case, except that Fe^+ and $FeCO^+$ were generated differently, the former being produced through laser ionization of a metal target, the latter by reaction of Fe^+ on acetone. In these experiments, molecular ions were typically irradiated for 0.5 to 0.6 s, and a surprising finding was that the IRMPD rate was not influenced by an Ar pressure in the ICR cell during the irradiation, whereas one could have thought that collisions with Ar would deactivate the vibrationally excited ions. As in the present case, Fe^+ ions were the only ion fragments observed by Freiser and co-workers using both CID and IRMPD at 944 cm^{-1} on Fe(i-butene)$^+$. In the case of Fe(1-butene)$^+$ and Fe(2-butene)$^+$, both $FeC_4H_6^+$ and Fe^+ fragments were observed under CID conditions, using low- and high-collision energy, respectively. However, only the loss of H_2 was observed by Freiser and co-workers using both SORI or IRMPD at 944 cm^{-1}. On the basis of these results, they concluded that the Fe(butadiene)$^+$ primary fragment might not absorb IR light at 944 cm^{-1}.

In the present experiments, however, Fe^+ fragments are observed when either Fe(1-butene)$^+$ or Fe(2-butene)$^+$ are irradiated. Figure 4 displays the corresponding parent and fragment ion relative intensities in the case of Fe(2-butene)$^+$. As can be seen in Figure 4, $Fe(C_4H_6)^+$ is the only fragment ion formed at high energies, Fe^+ fragments were only observed at low energy with a maximum at 950 cm^{-1}, and the situation is very similar in the case of Fe(1-butene)$^+$. The fact that two different fragments (Fe^+ and $Fe(C_4H_6)^+$) originating from the same parent ($Fe(C_4H_8)^+$) are formed with different relative abundance as a function of the wavelength could be interpreted different ways. This could suggest that the energy randomization is not complete prior to dissociation, but this is very unlikely; we have clear evidence for a complete energy randomization in molecular ion of the same size.[27] An alternative interpretation would be that Fe^+ is the product of a sequential process and results from the IR-induced dissociation of the primary fragment $Fe(C_4H_6)^+$.

To confirm this sequential fragmentation process and also to ascertain the structure of the $FeC_4H_6^+$ photofragments of

(54) Gauthier, J. W.; Trautman, T. R.; Jacobson, D. B. *Anal. Chim. Acta* **1991**, *246*, 211.

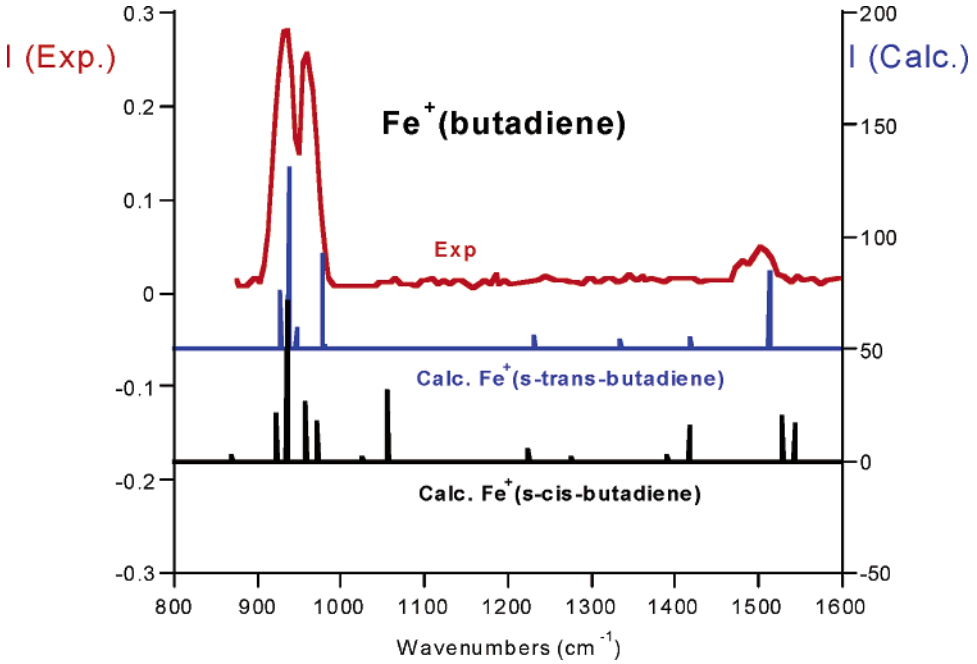

Figure 5. IRMPD spectrum of $FeC_4H_6^+$ (obtained by dehydrogenation of 2-butene by Fe^+) and calculated IR absorption spectra of Fe(s-*cis*-butadiene)$^+$ and Fe(s-*trans*-butadiene)$^+$ isomers.

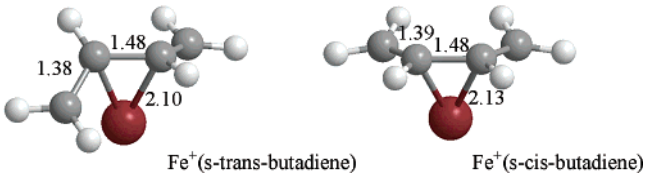

Figure 6. Geometrical structures associated to the lowest-energy states (quartet spin) of Fe(s-*cis*-butadiene)$^+$, and Fe(s-*trans*-butadiene)$^+$ isomers. Distances are given in angstroms.

Fe(1-butene)$^+$ and Fe(2-butene)$^+$, the IRMPD spectra of $FeC_4H_6^+$ ions generated either through dehydrogenation of 1-butene or 2-butene or by a ligand exchange reaction ($FeCO^+$ + butadiene) were recorded. The resulting IRMPD spectra appeared to be very similar. The IRMPD spectrum of the $FeC_4H_6^+$ ions produced through dehydrogenation of 2-butene by Fe^+ is given in Figure 5. One can observe a broad band with two maxima at 933 and 960 cm^{-1} and a weaker band at about 1500 cm^{-1}. Several isomers of $FeC_4H_6^+$ have been calculated, and the lowest-energy structure corresponds to an Fe^+ complexed by a butadiene preserving its s-trans geometry (Figure 6). This structure presents a quartet spin state and displays a C_2 symmetry. The lowest-energy structure for the Fe^+(s-*cis*-butadiene) presents a C_s symmetry and lies only 5.2 kcal/mol higher in energy (Figure 6). That is, the complexation to Fe^+ is slightly more favorable for the s-trans than for the s-cis isomer since the energy difference in the free ligand is 3.8 kcal/mol.

The comparison of the IRMPD spectrum of $FeC_4H_6^+$ to the calculated linear-IR absorption spectrum of the two isomers of Fe^+(butadiene) also given in Figure 5 also suggests that the $FeC_4H_6^+$ ions are present in the Fe^+(s-*trans*-butadiene) structure. Indeed, the calculated IR spectrum of Fe^+(s-*trans*-butadiene) displays two intense IR bands at 938 and 978 cm^{-1}, which could explain the IRMPD maxima at 933 and 960 cm^{-1}, respectively. The calculated IR band at 938 cm^{-1} corresponds to the CH_2 wagging, which is significantly blue-shifted as compared to that of the free ligand, and the other at 978 cm^{-1} corresponds to the CH bending mode. The calculated IR spectrum of the Fe^+(s-*cis*-butadiene) structure also presents a strongly IR active CH_2 wagging mode at 934 cm^{-1}, but the presence of two other bands at 957 and 971 cm^{-1} should lead to a broad band rather than two distinct bands as observed experimentally.

Besides the two main IRMPD bands at 933 and 960 cm^{-1} of $FeC_4H_6^+$, a small fragmentation yield was also observed at 1501 cm^{-1} (Figure 5), which could be assigned to the C═C stretching mode of one of the Fe^+(butadiene) isomers. No other IRMPD band was observed, especially near 1056 cm^{-1} where the Fe^+(s-*cis*-butadiene) isomer should present an IR active band according to the calculations. These results suggest that the IRMPD band at 1501 cm^{-1} can be assigned to the asymmetric C═C stretch of the Fe^+(s-*trans*-butadiene) isomer, which is calculated at 1513 cm^{-1} (Figure 5).

The above-described features of the IRMPD spectrum of $FeC_4H_6^+$ are perfectly in line with fragmentation patterns observed for both Fe(1-butene)$^+$ and Fe(2-butene)$^+$. These two complexes present IR absorption bands between 900 and 1000 cm^{-1}, and thus a first IRMPD process can lead to the loss of H_2. Then, the resulting $FeC_4H_6^+$ fragment ion can subsequently absorb IR light and eventually loses butadiene through a second IRMPD process. Furthermore, considering the position of the maximum yield, this also suggests that Fe^+ photofragments could be observed under irradiation with a CO_2 laser at 944 cm^{-1}. A sequential process could in principle also occur at higher energy since both Fe(1-butene)$^+$ and Fe(2-butene)$^+$, on one hand, and $FeC_4H_6^+$ on the other, present IR active vibrational transitions. Nevertheless, the efficiency of the IRMPD process for Fe(butadiene)$^+$ around 1501 cm^{-1} is probably not sufficient to allow for a dissociation of $FeC_4H_6^+$ into Fe^+ and C_4H_6.

5. Concluding Remarks

Gas-phase organometallic complexes of hydrocarbons have been characterized by infrared spectroscopy. Overall, a very

good agreement was found between the experimental IRMPD spectrum of the mass-selected ions and the calculated IR absorption spectrum of the corresponding lowest-energy isomer. This work shows that three selectively prepared isomers of Fe^+(butene) present different IRMPD spectra. In good agreement with the corresponding calculated IR spectra, the lower-energy part (800−1000 cm^{-1}) of the IRMPD spectra of Fe^+(i-butene), Fe^+(2-butene), and Fe^+(2-butene) are different. Fe^+(butadiene) ions have been selectively prepared, and the IRMPD features suggest that the butadiene preserves its s-trans structure upon complexation. This result is in good agreement with the calculations, which predict this structure to be lower in energy than the Fe^+(s-*cis*-butadiene) isomer. In all these cases, despite the complicated multiphotonic nature of the IRMPD, this process yields to an IR spectrum presenting the main features of the corresponding IR absorption spectrum.

This study further confirms the potential of the IRMPD spectroscopy exploiting the brightness and the wide tunability of the infrared free-electron laser for characterizing the structures of gas-phase molecular ions under FTICR-MS conditions through their vibrational fingerprints. This particular infrared spectroscopy is a very powerful tool to characterize selectively prepared molecular ions using an FTICR mass spectrometer. This type of experimental setup, which can be coupled to a variety of ion sources, would allow for the structural identification of a large variety of ions. Ions of biological interest could be accessed by using MALDI or ESI. IRMPD spectroscopy of selectively prepared highly reactive ionic species under FTICR-MS conditions would also provide an alternative method of characterization to the IR spectroscopy of these species isolated in rare gas matrixes, where the largest shifts are observed with cationic systems.[55] Finally, the FTICR-MS technique is also particularly well-suited for the studies of reaction mechanisms, and one should be able to characterize the structures of mass-selected reactive intermediates, which is likely to have a large impact in the field of organometallic catalysis in the gas phase.

Acknowledgment. This work was supported by the CNRS and the Laser Center POLA at the University of Paris-Sud 11. We would like to thank our colleagues (Michel Heninger, Gérard Bellec, and Gérard Mauclaire) who, together with two of us (P.B. and J.L.), developed the mobile FTICR mass spectrometer used in this work. We also would like to thank the CLIO team, and particularly François Glotin, for help and support, as well as Luke MacAleese for helpful discussions and proofing of this manuscript.

JA0488176

(55) Zhou, M.; Andrews, L.; Bauschlicher, C. W., Jr. *Chem. Rev.* **2001**, *101*, 1931.